Design and implementation of antihandshaking position control for a voice coil motor

Shir-Kuan Lin, Chao-Min Wang, and Shyh-Jier Wang

Citation: Journal of Applied Physics **103**, 07F128 (2008); doi: 10.1063/1.2839338
View online: http://dx.doi.org/10.1063/1.2839338
View Table of Contents: http://scitation.aip.org/content/aip/journal/jap/103/7?ver=pdfcov
Published by the AIP Publishing

Design and implementation of antihandshaking position control for a voice coil motor

Shir-Kuan Lin,[1,a)] Chao-Min Wang,[1] and Shyh-Jier Wang[2]
[1]*Department of Electrical and Control Engineering, National Chiao Tung University, 1001 Ta Hsueh Road, Hsinchu City 30010, Taiwan*
[2]*Delphi Taiwan Ltd., 4F, 471, Sec. 2, Pa Teh Road, Hu Kou, Hsin Chu Hsien 303, Taiwan*

(Presented on 8 November 2007; received 11 September 2007; accepted 11 January 2008; published online 21 March 2008)

This paper deals with the position control of the voice coil motor (VCM) with handshaking. A disturbance observer is proposed to estimate the low-frequency handshaking disturbance, so that a handshaking-robust controller can be constructed. While a handshaking stabilizer can compensate for the vibration of the whole lens set, a robust controller is still required to precisely hold the autofocusing lens by rejecting the handshaking disturbance. To meet the request of miniaturization, the control is implemented on a field programmable gate array chip. © *2008 American Institute of Physics*. [DOI: 10.1063/1.2839338]

I. INTRODUCTION

Recently, a voice coil motor (VCM) has been used in the autofocusing (AF) system of a commercial digital camera to meet the trend of miniaturization.[1] Some works[2–5] proposed the design methods for the VCM, while Yu *et al.*[1] developed the adaptive model following control (AMFC) to overcome the loading variation due to the posture change of a camera. However, the AF system must also operate well under handshaking, which was not taken into account in the work.[1] The handshaking induces low-frequency disturbance to the AF system. This paper deals with the robust control of the AF system to reject external disturbances, especially the one induced by handshaking. The controller proposed in this paper utilizes the disturbance observer to estimate the external disturbance and then to compensate for it. The disturbance observer[6] has been proven to work well.[7,8]

II. VOICE COIL MOTOR

In the camera AF system, a lens holder carrying the optical focusing lens is driven by the moving coil of the VCM, as shown in Fig. 1.

As the VCM moves the lens holder, the MR sensor generates two sinusoidal signals with a 90° phase shift. The position estimation algorithm proposed by Yu *et al.*[1] is used to transform the MR signals into the position of the lens holder. The 0.8 mm polar pitch of the MR encoder is divided into four regions according to the one of the MR signal with $\sin\theta_e$ (denoted by x_{NA}). The other one of $\cos\theta_e$ is denoted by x_{NB}. Region 1 begins from $\theta_e=-1/4\pi$ to $+1/4\pi$. The other three regions follow one by one with a range of $\frac{1}{2}\pi$ for each. Let $s=x_{\mathrm{NA}}, -x_{\mathrm{NB}}, -x_{\mathrm{NA}}$, and x_{NB} for θ_e in regions 1–4, respectively. The position (denoted by p) of the lens holder was expressed in the work of Yu *et al.*[1] as

$$p = 0.2n + (0.1 + 0.1414s)\ \mathrm{mm}, \tag{1}$$

where n is the number of regions that the VCM have passed.

III. PROPOSED CONTROLLER

To overcome the varying handshaking disturbance, a disturbance observer is incorporated with the PI, so that the disturbance can be dynamically estimated and then be compensated for. By taking into account the saturation of the plant, an antiwindup strategy[9] is introduced in the PI controller. The block diagram of the overall control is shown in Fig. 2.

The proposed disturbance observer uses the control effort f and the measured VCM velocity v (with the measurement noise δ) to estimate the uncertainty n_d. It is desired that the output estimate e_0 of the disturbance observer approaches n_d as the time t approaches infinity. As a result, f will compensate for n_d, so that the plant velocity v will follow $G_p(s)u$. A simple concept is to introduce the inverse of the nominal plant P_n of the plant G_p. Ideally, the difference of f and $P_n^{-1}(s)v$ is the uncertain disturbance n_d. However, the estimation error comes from the high-frequency measurement noise δ. Thus, a low-pass filter Q is required to eliminate this noise. This is verified mathematically in the following.

Let $G_{uv}(s)$, $G_{n_dv}(s)$, and $G_{\delta v}(s)$ be the transfer functions of

$$G_{uv}(s) \equiv \frac{v(s)}{u(s)} = \frac{G_p(s)[P_n(s)]}{P_n(s) + [G_p(s) - P_n(s)]Q(s)}, \tag{2}$$

$$G_{n_dv}(s) \equiv \frac{v(s)}{n_d(s)} = \frac{G_p(s)P_n(s)[1 - Q(s)]}{P_n(s) + [G_p(s) - P_n(s)]Q(s)}, \tag{3}$$

$$G_{\delta v}(s) \equiv \frac{v(s)}{\delta(s)} = \frac{-G_p(s)Q(s)}{P_n(s) + [G_p(s) - P_n(s)]Q(s)}. \tag{4}$$

It is then easy to obtain

$$v = G_{uv}(s)u + G_{n_dv}(s)n_d + G_{\delta v}(s)\delta. \tag{5}$$

It follows from Eqs. (2)–(5) that $G_{uv}(s)\approx P_n(s)$, $G_{n_dv}(s)\approx 0$, and $G_{\delta v}(s)\approx -1$ as $Q(s)\to 1$. Since $Q(s)\to 1$ at low frequencies, $G_{n_dv}(s)\approx 0$ implies that the disturbance n_d should not affect the plant output v in the low-frequency

a)Author to whom correspondence should be addressed. Electronic mail: sklin@mail.nctu.edu.tw.

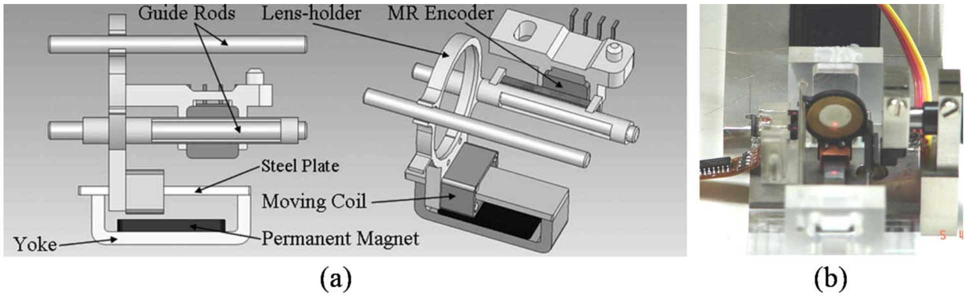

FIG. 1. (Color online) Voice coil motor in an autofocusing system: (a) component illustration and (b) photo.

operation, while $G_{uv}(s) \approx P_n(s)$ means that the transfer function of the plant velocity v over the input u remains the same as the original one without the disturbance observer. Moreover, $G_{\delta v}(s) \approx -1$ indicates that the measurement noise affects the velocity v in a negative form. Fortunately, the frequency of the noise δ is much higher than the bandwidth of the mechanical system of the VCM; its effect will not appear in the dynamics of the VCM.

When the VCM operates at high frequencies, we have $Q \to 0$ so that $G_{uv}(s) \approx G_p(s)$, $G_{n_d v}(s) \approx G_p(s)$, and $G_{\delta v}(s) \approx 0$. The observer rejects the noise δ, but the disturbance n_d affects the velocity v. It is then not recommended to apply such a control scheme in the high-frequency operation.

Rather than those chosen in the previous works,[7,8] we use a simple second-order low-pass filter of

$$Q(s) = \frac{1}{(\tau s)^2 + 2\xi \tau s + 1}, \tag{6}$$

where ξ is the damping ratio and τ is the cutoff frequency of the filter. It is suggested to choose ξ as 0.707, so that τ is exactly the bandwidth of the transfer function [Eq. (6)].

Kempf and Kobayashi[7] pointed out that the cutoff frequency τ of the filter is constrained by the sampling time. A smaller sampling time allows a larger value of τ.

IV. FPGA IMPLEMENTATION

The nominal plant of the VCM can be described in the form of[1]

$$P_n(s) = \frac{K_f}{(Ls + R)(ms + B_m)}, \tag{7}$$

where L is the coil inductance, R is the coil resistance, m is the mass of the VCM moving part, B_m is the damping constant, and K_f is the force constant of the driver. The control hardware system is a FPGA chip incorporated with an analog to digital (A/D) converter and a digital to analog (D/A) converter. The MR signals of the VCM are inputted into the FPGA through the A/D converter, while the output of the controller is sent to the D/A converter, which generates the voltage for the moving driver of the VCM. The three main blocks of the FPGA (see Fig. 3) are devoted to the position estimation algorithm, antiwindup PI controller, and the disturbance observer, in addition to the A/D and the D/A blocks.

Figure 3(a) shows the FPGA block (denoted by PEA) for the position estimation. The system clock signal clk_system is 50 MHz, while the sampling is triggered per 81.92 μs by the signal clk_sample. The PEA block takes the signals X_NA and X_NB from the A/D converter per system clock. Comparing X_NA and X_NB with $\left(\pm\frac{1}{4}\pi\right)$ yields the electrical region (denoted by Rg) of θ_e. For instance, if X_NA $\geqslant 1/4\pi$, θ_e is at region 2, so let $s=-$X_NB in Eq. (1) and Rg=2. Moreover, if Rg is changed, n in Eq. (1) is also updated accordingly. Finally, the position p is calculated using Eq. (1) and the velocity v is obtained by the backward difference approximation.

The antiwindup PI controller handles the velocity control and is implemented in the block antiwindup_PI_Controller [see Fig. 3(b)]. However, there is another P_Controller block in its upstream, which deals with the position control, i.e., calculates $K_{dp}(r_d - d)$ as the output com_v. In these two blocks, both signals p and v are captured per sampling clock from the PEA block. The PI block performs the following computation:

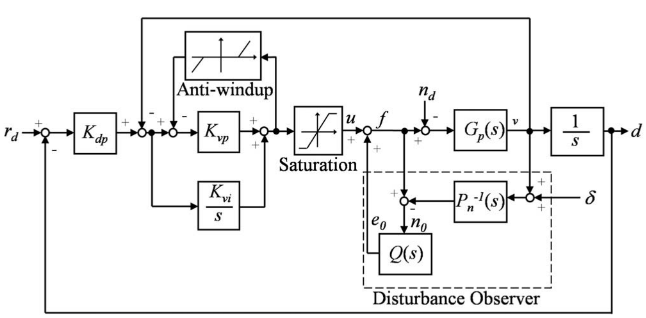

FIG. 2. Antiwindup PI controller with a disturbance observer.

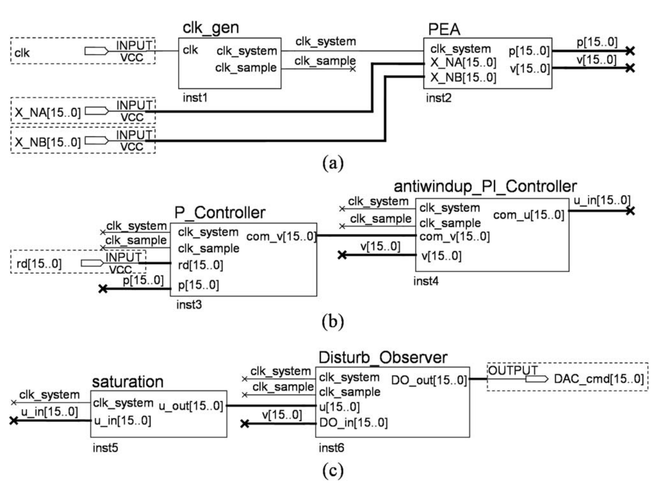

FIG. 3. (Color online) FPGA implementation: (a) position estimation block, (b) antiwindup PI block, and (c) disturbance observer block.

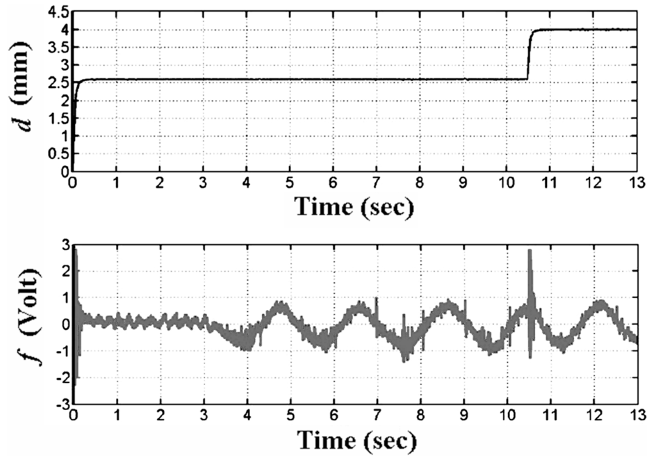

FIG. 4. (Color online) Experimental results of the proposed control scheme: (a) position measured by the LDM and (b) control effort recorded by the oscilloscope.

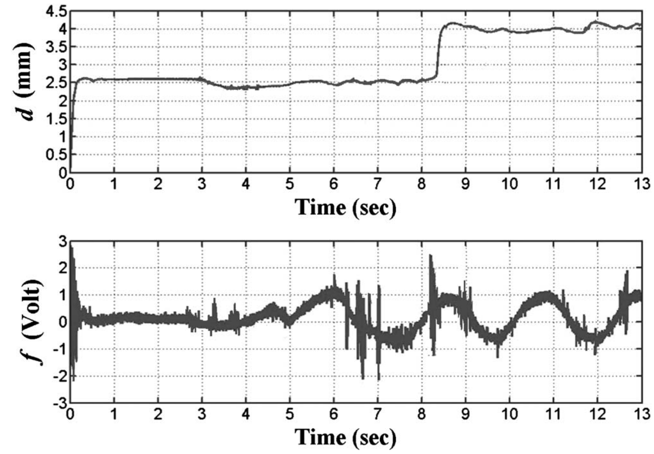

FIG. 5. Experiment results of the AMFC scheme: (a) position measured by the LDM and (b) control effort recorded by the oscilloscope.

$$u_c = u_c + K_{vi} e_v t_s + K_{vp}(e_v - v_a), \tag{8}$$

where e_v=com_v$-v$, t_s is the sampling time, u_c is the output signal com_u (or u_in), and v_a is the output of the antiwindup. The compensation value v_a is the result of multiplying the excess of u_c over the saturation limit with the gain K_a (see Ref. 9).

The output of the PI controller is constrained by the saturation block before entering the disturbance observer block Disturb_Observer [see Fig. 3(c)]. The transfer function of the disturbance observer in Fig. 2 is equivalent to

$$e_0(s) = \frac{1}{1-Q(s)}\left[u(s) - \frac{Q(s)}{P_n(s)}v(s)\right] = \left(1 + \frac{1}{\tau^2 s^2 + 2\xi\tau s}\right) \times \left[u(s) - \frac{(Ls+R)(ms+B_m)}{K_f(\tau^2 s^2 + 2\xi\tau s + 1)}v(s)\right], \tag{9}$$

where $u(s)$ is the output of the saturation block and $e_0(s)$ is that of the disturbance observer. Let $v_1=(ms+B_m)v$ and $v_2=[(Ls+R)/K_f]v_1$. It is then easy to obtain v_1 and v_2 by the backward difference approximation. Define $x=v_2/(\tau^2 s^2+2\xi\tau s+1)$ to transform the problem into a second order differential equation of $\tau^2\ddot{x}+2\xi\tau\dot{x}+x=v_2$. The three step Adams–Bashforth numerical method is implemented to solve x. The transfer function $1/(\tau^2 s^2+2\xi\tau s)$ is also implemented in a similar manner.

V. EXPERIMENTS

In the experiments, L=1.2 mH, R=32.8 Ω, m=1.8 g, B_m=0.005 N/(m s), and K_f=42.3 gW/A. The sampling time is set as 81.92 μs and the cutoff frequency τ of the low-pass filter $Q(s)$ is chosen as 754 rad/s or 120 Hz. On the other hand, the gains of the PI antiwindup controller are K_{dp}=20, K_{vp}=2.5, and K_{vi}=1.2, and the maximum value for the saturation is u_{max}=4.7 V. The AF system is harmonically shaken by two hands that hold the AF system.

Figure 4 shows one of the experimental results for the control with the disturbance observer, in which the two target commands are 2.5 and 4 mm, respectively. It can be seen from Fig. 4 that there are no fluctuations in the steady states, so that this control scheme is robust to the handshaking disturbance. However, the manufacturing precision of the VCM still makes steady-state errors, i.e., the steady-state errors are 16 and 11 μm.

In the first 3 s of Fig. 5, the steady-state error of the AMFC is almost as small as that of the controller with the disturbance observer since there is no handshaking. However, the position of the AMFC system fluctuates about 300 μm under the situation of handshaking. This comparison shows that the disturbance observer is superior to the AMFC in the estimation and compensation of the dynamical disturbance.

VI. CONCLUSIONS

This paper proposes an antiwindup PI controller incorporated with the disturbance observer to control the VCM. A simple second order low-pass filter is used in the disturbance observer, which is verified good enough to estimate the handshaking disturbance.

ACKNOWLEDGMENTS

This work was supported by the National Science Council of Taiwan under Grant No. NSC 95-2221-E-009-101.

[1]H. C. Yu, T. Y. Lee, S. K. Lin, L. T. Kuo, S. J. Wang, J. J. Ju, and D. R. Huang, J. Appl. Phys. **99**, 08R901 (2006).
[2]Y. Hirano, J. Naruse, and R. Tsuchiyama, IEEE Trans. Magn. **25**, 3073 (1989).
[3]H. C. Yu, T. Y. Lee, S. J. Wang, M. L. Lai, J. J. Ju, D. R. Huang, and S. K. Lin, IEEE Trans. Magn. **41**, 3979 (2005).
[4]P. C. P. Chao and S. C. Wu, IEEE Trans. Magn. **43**, 2579 (2007).
[5]C. W. Chiu, P. C. P. Chao, and D. Y. Wu, IEEE Trans. Magn. **43**, 2582 (2007).
[6]T. Umeno and Y. Hori, IEEE Trans. Ind. Electron. **38**, 363 (1991).
[7]C. J. Kempf and S. Kobayashi, IEEE Trans. Control Syst. Technol. **7**, 513 (1999).
[8]M. T. White, M. Tomizuka, and C. Smith, 1999 Proceedings of the American Control, 1999 (unpublished).
[9]G. F. Franklin, J. D. Powell, and A. Emami-Naeini, *Feedback Control of Dynamic Systems* (New Jersey, Prentice-Hall, 2002).